ELECTRONIC SUPPLEMENT

Interhemispheric space-time attributes of the Dansgaard-Oeschger oscillations between 0-100 ka

Linda A. Hinnov
Morton K. Blaustein Department of Earth and Planetary Sciences
Johns Hopkins University, Baltimore, Maryland USA
e-mail: hinnov@jhu.edu

Michael Schulz
Institut für Geowissenschaften, Universität Kiel
Olshausenstr. 40, D-24118 Kiel, Germany

Pascal Yiou
Laboratoire des Sciences du Climat et de l'Environnement
UMR CEA-CNRS, CE Saclay l'Orme des Merisiers, 91191 Gif-sur-Yvette, France

PART 1. Spectrogram design; supplementary spectrograms

Spectrograms are classically displayed as a running Fast-Fourier Transform (FFT) of a time series. Variants of the technique have now been used with great success in the analysis of paleoclimatic time series for purposes of quantifying unstable sediment accumulation and/or tracking quasi-periodic paleoclimatic signals forced by Earth's orbital parameters (e.g., Yiou et al. 1991). We decided to construct our spectrograms using MTM harmonic analysis (e.g., Meyers et al. 2001), and display the results in two parts, as amplitude (or line) spectra, and as F-statistic probabilities output from the harmonic line test of Thomson (1982). Our procedure:

- Interpolate time series linearly to $\Delta t = 4$ year uniform sample rate (arbitrary).
- Using three 2π multitapers and adaptive weighting, calculate line spectra over 6 kyr windows with a 2 kyr increment (67% overlap), over f = [0, 2 cycles/kyr]. The output spectral line estimates have an elementary bandwidth resolution of f = 0.167 cycles/kyr and have ca. 6 degrees of freedom (or less, depending on the adaptive weighting).
- Record the amplitudes of the line spectra and their F-statistic probabilities, which are calculated by numerical integration of the F-distribution with ca. 6 degrees of freedom (or less, determined by the adaptive weighting procedure).
- Apply the Matlab™ "surf" graphics display routine, plotting the line spectra in 3D, and the F-statistic probabilities as 2D contours.

Spectrograms of the North Atlantic Core MD95-2042 planktonic and benthic $\delta^{18}O$ records and $\delta^{18}O_{ice}$ of Byrd Station, Antarctica appear in **Figures S1** and **S2**.

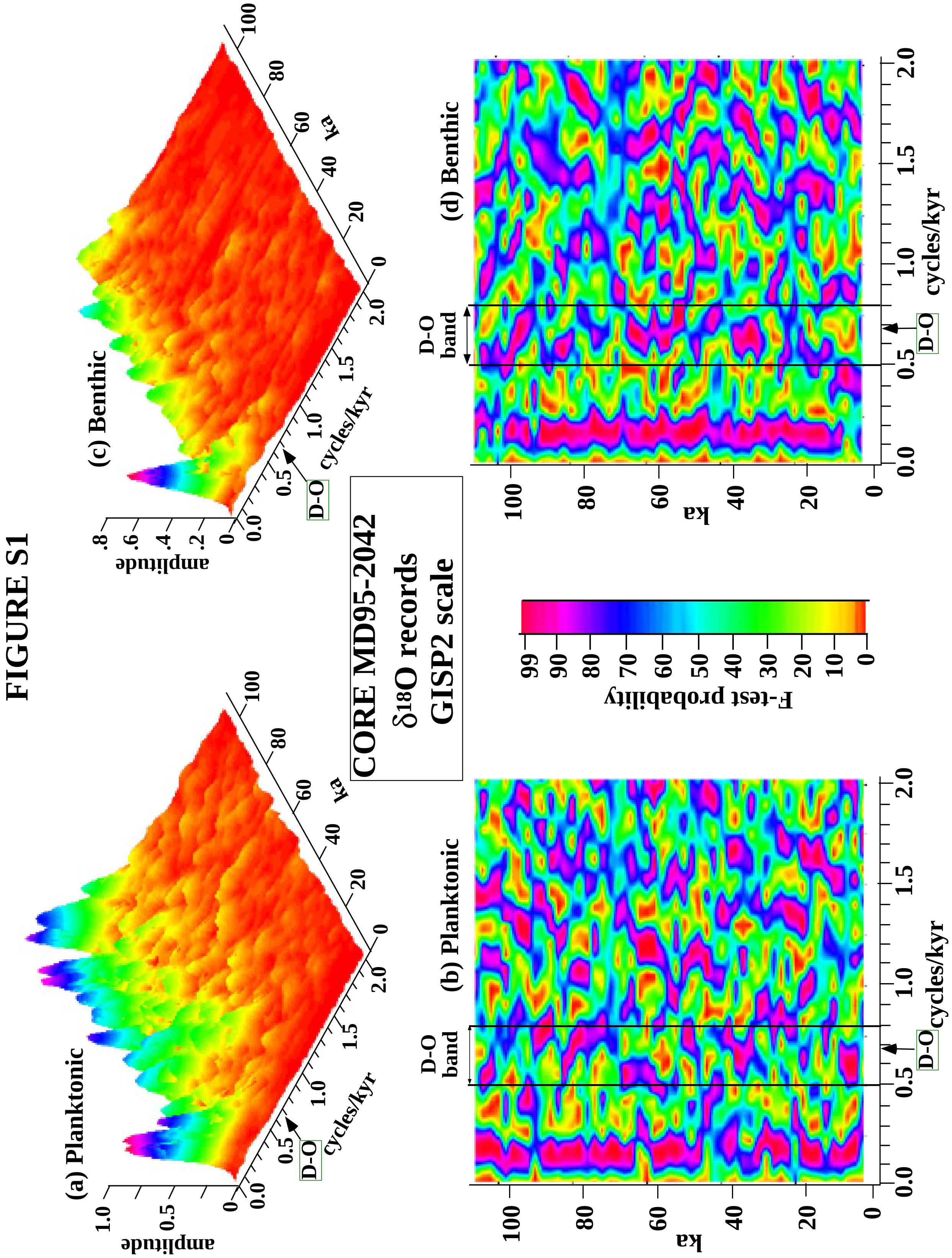

Figure S1. Spectrogram analysis of planktonic and benthic $\delta^{18}O$ from Core MD95-2042 over 0-100 ka. Design parameters are given in **PART 1**. (a) Line spectra of the planktonic record, where amplitude is in per mill $\delta^{18}O$; (b) Adaptive-weighted F-statistic probabilities of the lines computed in (a); (c) Line spectra of the benthic record, where amplitude is in per mill $\delta^{18}O$; and (d) adaptive-weighted F-statistic probabilities of the lines computed in (c). The passband of the Taner-Hilbert analyses presented in **Figure 6** of the main paper is indicated in (b) and (d). Arrows labeled D-O indicate the mean D-O frequency f=1/1.47 cycles/kyr. All spectrograms have an elementary bandwidth resolution of Δf=0.167 cycles/kyr.

Figure S2

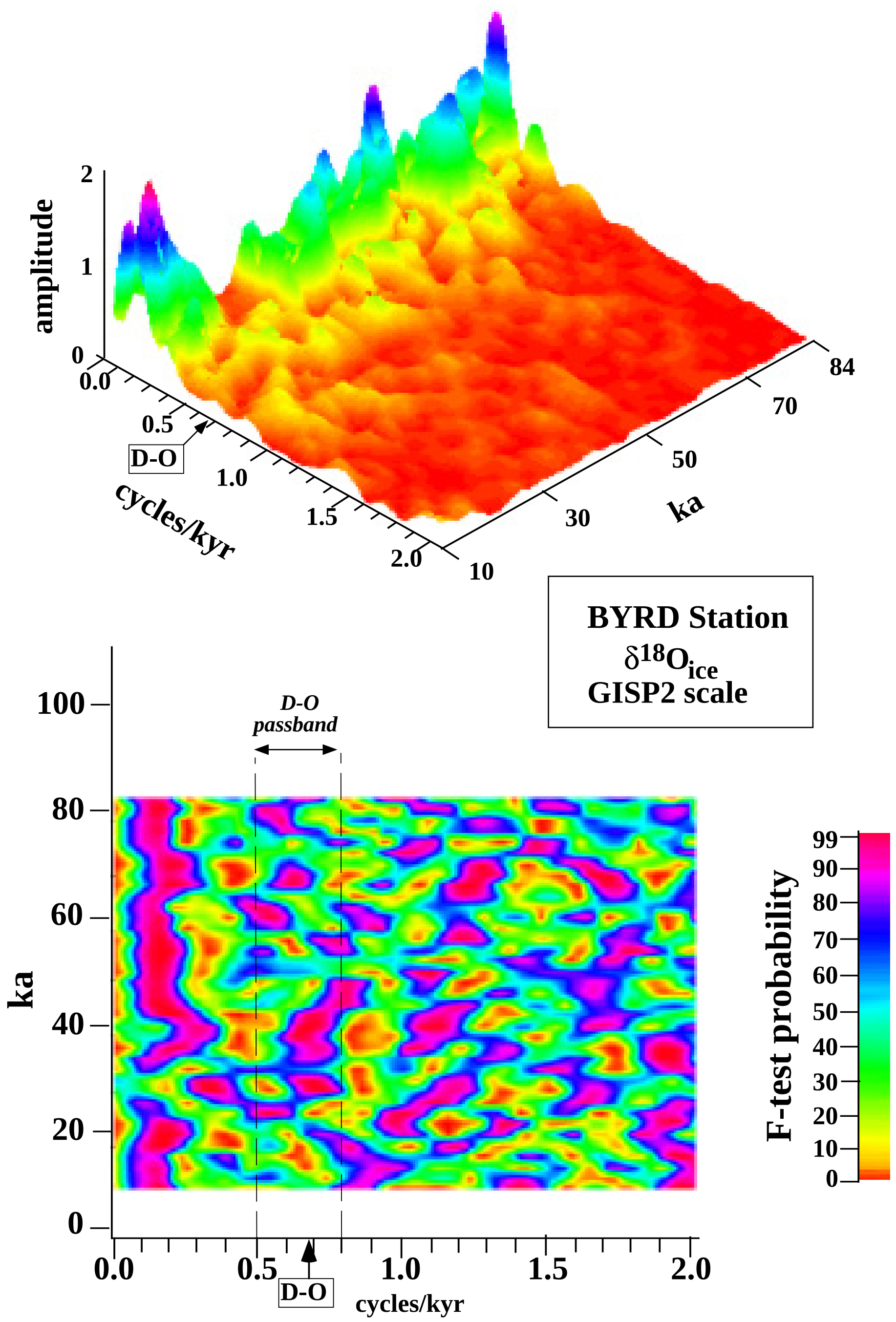

Figure S2. Spectrogram analysis of $\delta^{18}O_{ice}$ from Byrd Station over 10-90 ka. Design parameters are given in the **PART 1**. (a) Line spectra of the record, where amplitude is in per mill $\delta^{18}O_{ice}$; (b) Adaptive-weighted F-statistic probabilities of the lines computed in (a). The passband of the Taner-Hilbert analyses presented in **Figures 5** and **6** of the main paper is indicated indicated in (b). Arrows labeled D-O indicate the mean D-O frequency f=1/1.47 cycles/kyr. The elementary bandwidth resolution is Δf=0.167 cycles/kyr.

PART 2. Ferraz-Mello analysis

Temporal changes in amplitude and phase of 1470-year signal components are estimated by a modified harmonic-filtering algorithm (Ferraz-Mello 1981), which generates a sinusoidal filter function by fitting a sine-wave of given period and variable amplitude and phase to a time series. The method allows the direct processing of unevenly spaced time series. To obtain time-dependent estimates, the time series is split into overlapping segments, using a sliding window of width 4 x 1470 year. Each segment is linearly detrended prior to tapering with a Welch-Shape-1 window (e.g., Schulz & Stattegger 1997). The selected window width offers a good compromise between statistical and systematic errors and results in a half-amplitude bandwidth of approximately 0.26 cycles/kyr. Note that due to the finite window width, a step-like amplitude increase appears 4×1470 year wide.

PART 3. Complex signal analysis

Complex, or quadrature, signal analysis is a classical technique used to estimate frequency, amplitude and phase attributes of a real signal as a function of time (e.g., Bracewell 1965). Processing information is outlined in detail by Taner et al. (1979), in which the complex representation of a real signal g(t), i.e., $G(t) = g(t)+ig^*(t)$, with $i^2 = -1$, is obtained by Hilbert transformation. The attributes of the complex signal are:

Instantaneous amplitude: $A(t) = |G(t)|$
Instantaneous phase: $\theta(t) = \arctan[g^*(t)/g(t)]$
Instantaneous frequency: $f(t) = d\theta(t)/dt$

The data of the present study are highly “colored” time series with a high dynamic range, particularly those from the Southern Hemisphere, and so it was necessary to isolate the D-O signal first by bandpass filtering. Thus, the precision and accuracy of the signal attribute estimates are dependent upon the parameters of the applied bandpass filter. The procedure:

- Interpolate the time series to a uniform spacing of Δt=4 years.
- Apply Taner bandpass filter (see **Electronic Supplement -PART 4**).
- FFT the bandpassed time series g(t) (we used the radix transform of Singleton (1969).
- Zero out the coefficients of the negative sampled frequencies; double the coefficient values of the positive frequencies.
- Inverse FFT to obtain G(t).
- Calculate A(t) and $\theta(t)$. (Notes: Singleton's FFT requires multiplying $g^*(t)$ by –1, and the four quadrant complex arctangent FORTRAN function "atan2" to calculate $\theta(t)$.)
- Unwrap $\theta(t)$ using the Matlab™ "unwrap" utility, and calculate f(t) by numerical differencing (to obtain cycles/year, divide by 2π).

The efficacy of the procedure is illustrated in **Figure S3**, in which the attributes of 1470-year periodic signal $g(t_n)$ experiencing a 40000-year frequency modulation and a 20000-year amplitude modulation over a 100000-year interval. This signal was calculated by sampling a sinusoid $h(t_n)$ of period 1/1.47 cycles/kyr at intervals $t'_n=n\Delta t$, with Δt=4 years, and n=1, 2, ..., 25000; this was modulated by $A(t'_n) = \sin[2\pi t'_n/(20000 \text{ years})]$, such that $g(t'_n) = A(t'_n)\cdot h(t'_n)$. For the frequency modulation, the timescale t'_n was replaced with $t_n=t'_n+\Delta t[1+\sin(2\pi t'_n/40000 \text{ years})]$, to give $g(t_n)$; then resampled to a uniform rate of Δt=4 years. Of special note is that the amplitude modulation imposes "singularities" in f(t) whenever it passes through zero (causing discontinuities in the instantaneous phase). Such "singularities" can also picked up by depositional hiatuses or other perturbations not related to amplitude forcing, and can also occur artifactually as the result of imposed passbands.

FIGURE S3

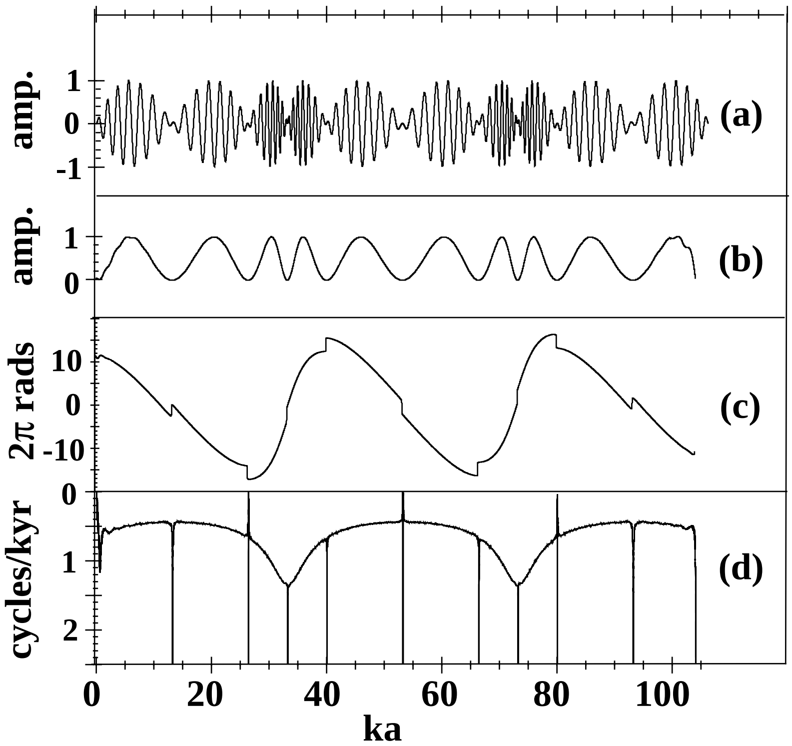

Figure S3. Performance of Hilbert complex signal analysis on the discrete amplitude and frequency modulated time signal $g(t_n)$. (a) The modulated signal; (b) instantaneous amplitude $A(t_n)$; (c) instantaneous phase $\theta(t_n)$; and (d) instantaneous frequency $f(t_n)$.

PART 4. The Taner bandpass filter

We elected to use a Ricker-like filter originally designed to process seismic traces (Taner 2000). The bandpass form of the Taner filter satisfies IEEE standards for filter design, and is as follows:

$$T_b(x)=\beta\cdot\{\exp[\alpha(x_L-x)] + \exp[\alpha\,(x-x_H)]\}$$

where $x = \ln(f)/\ln(2)$, x_L and x_H are user-specified low and high cutoff frequencies in octave space, f has units of cycles/time-unit, $\beta = 0.5\cdot\ln(0.5)$, and $\alpha = \ln[(-3.0103\text{-}D/10)\cdot\ln 10/\beta]$ with D the user-specified roll-off rate in decibels/octave.

The impulse response of the Taner filter used in our study is illustrated in **Figure S4**. We selected the cutoff frequencies f_L=0.5 cycles/kyr, and f_H=0.8 cycles/kyr, after consulting the GRIP and GISP2 probability spectrograms (see **Figure 3**, main text), with D=10^{12} dB/octave.

FIGURE S4

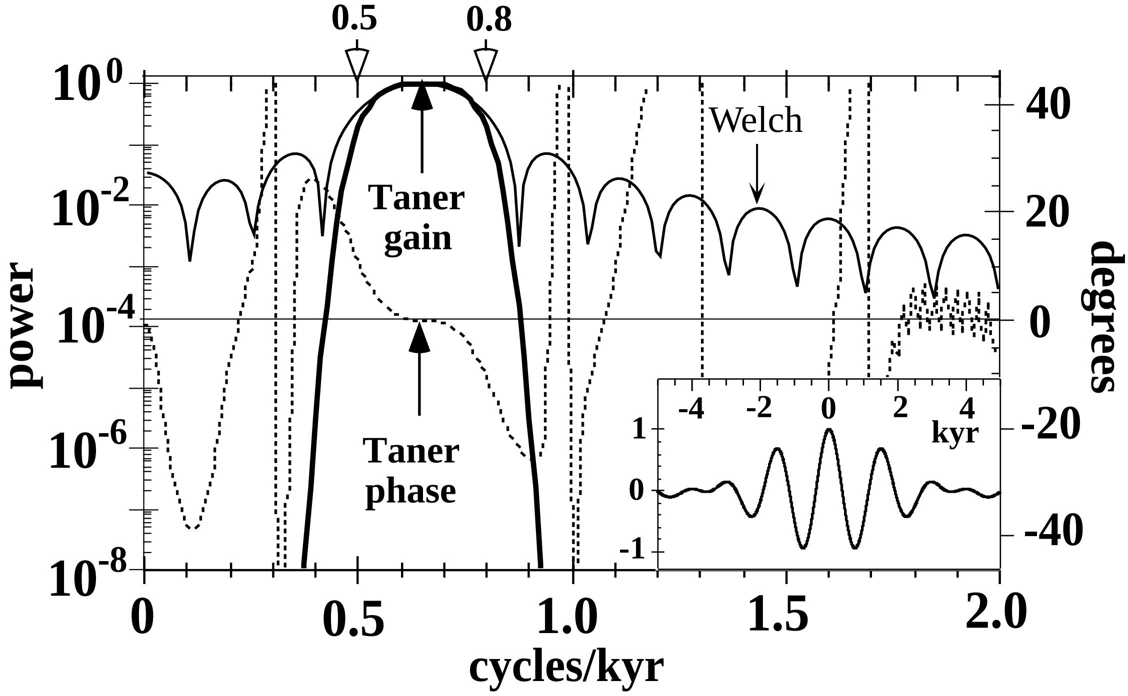

Figure S4. Frequency impulse response of the Taner filter, with cutoff frequencies f_L=0.50 cycles/kyr and f_H=0.80 cycles/kyr, and a rolloff rate of D=10^{12} decibels/octave; also shown is the gain of the Welch filter used in the Ferraz-Mello analysis. Time response is shown in the inset (lower right): note the rapid tailing of the Ricker-like filter over ca. four average D-O cycles.

REFERENCES –

Bracewell, R.N. (1965), *The Fourier Transform and its Applications*, McGraw-Hill Book Co., New York.

Ferraz-Mello, S. (1981), Estimation of periods from unequally spaced observations, *Astronomical Journal*, **86**, 619-642.

Meyers, S., Sageman, B., and Hinnov, L.A. (2001), Integrated quantitative stratigraphy of the Cenomanian-Turonian Bridge Creek Limestone member using evolutive harmonic analysis and stratigraphic modeling, *Journal of Sedimentary Research*, **71**, 627-643.

Schulz, M. and Stattegger, K. (1997), SPECTRUM: spectral analysis of unevenly spaced paleoclimatic series, *Computers in Geosciences*, **23**, 929-945.

Singleton, R.C. (1969), An algorithm for computing the mixed radix fast Fourier transform, IEEE Transactions on Audio and Electroacoustics, **17(2)**, 93-103.

Taner, M.T. (2000), Attributes revisited, *Technical Publication, Rock Solid Images, Inc*., Houston, Texas, URL: http://www.rocksolidimages.com/pdf/attrib_revisited.htm.

Taner, M.T., Koehler, F., and Sheriff, R.E. (1979), Complex trace analysis, *Geophysics*, **44(6),** 1041-1063.

Thomson, D. (1982), Spectrum estimation and harmonic analysis, *Proceedings of the IEEE*, **70**, 1055-1096.

Yiou, P., Genthon, C., Ghil, M., Jouzel, J., Le Treut, H., Barnola, J., Lorius, C., and Korotkevitch, Y. (1991), High-frequency paleovariability in climate and CO_2 levels from Vostok ice core records, *Journal of Geophysical Research*, **96**, 20365-20378.